ISSN No:-2456-2165

Reinterpretation of aeromagnetic data and contribution to the structural study of the Western part of Kipushi territory in DR Congo

Fulgence MULOPO SHINGINYEKA[1], Eli-Achille MANWANA MFUMUKANI[2], Jean LUKUSA[3].

[1]Department of Physics and Applied Sciences, National Pedagogical University, Kinshasa, DR Congo.
[2]Department of Internal Geophysics, Center of Research in Geophysics (CRG), Kinshasa, DR Congo.
[3]Department of Applied Geology, Geological and Mining Research Center (CRGM), Kinshasa, DR Congo.

Abstract:- The mineralization of the Kipushi territory in the Haut Katanga Province in DR Congo has propagated in the surrounding formations along the places where faults meet with lithostratigraphic contacts which seem to be very complex to interpret by direct observation methods. This is how, to overcome this problem, we reinterpreted the old airborne magnetic data that were digitized with the help of new software. The raw data obtained were processed using regional-residual separation methods, derivatives and analytical signal. We observed very high magnetic anomalies but also very fluctuating in the western part of our study area, which allowed us to identify magmatic intrusions as well as several faults which testify to the presence of an intense tectonic activity in this zone. On the other hand, the eastern part is characterized by medium and / or high anomalies varying very slowly. We have established a lineament map that is most certainly related to the mineralization of this zone. The majority of identified lineaments are found in the Roan, Nguba and Kundelungu Groups while others along their contacts. The depth of most of the identified contacts, faults and dykes has been estimated to be less than 1000 m using Euler's deconvolution and Peters half-slope methods.

Keywords:- *Magnetic Data, Structural Interpretation, Lineaments, Mineralization, Kipushi.*

I. INTRODUCTION

The beginnings of the geological study of Katanga province date back to 1892 with the expedition of Jules Cornet. About ten years later, the prospecting of the 'Tanganyika Concessions Limited' followed, then from 1906 the studies of the 'Union Minière du Haut-Katanga' extended into the interwar period by the work of the Special Committee of Katanga and continued from 1967 under the banner of 'Générale des Carrières et des Mines (Gécamines)' (François, A., 2006 [1]). At the same time and until today, academic research and, more recently, private mining companies work to refine and update geological knowledge. It is with this in mind that we carried out this geophysical study, which is based on the processing and interpretation of magnetic data from the aeromagnetic survey carried out by the Hunting company in 1970 in the territory of Kipushi. This with the aim of improving knowledge of the structural geology of this region by bringing some interesting additions to the geological cartography. Indeed, according to the 'Cellule Technique de Coordination et de Planification Minière (CTCPM)', 2003 [2], the main minerals found in this area are copper, cobalt, tin, uranium, iron, molybdenum, etc. therefore, most rocks and geological structures containing these minerals have magnetic signatures that distinguish them from their environment. Magnetic maps will therefore be of utmost importance in this case as they will be useful in locating and identifying these geological structures hidden beneath the earth's surface. This study will thus make it possible to guide geologists in their investigation with a view to the discovery of new mineral deposits in this area.

II. MATERIAL AND METHOD

2.1. MATERIAL

In addition to an important magnetic and geological database of the study area, we used software such as Geosoft Oasis montaj, ArcGis, Golden Surfer and RockWorks allowing digitization, analysis, processing and data modeling. This software has enabled us to perform various data processing, to present the results in the form of maps and to interpret them.

2.2. METHOD

This work aims to analyze, process and interpret the aeromagnetic data in order to highlight the different geological structures that may be related to the mineralizations in the territory of Kipushi. The method used to carry out this study can be summed up in three steps:

- The first step is the digitization of the old maps acquired during the aeromagnetic survey carried out by the Hunting company in 1970 and the creation of a database of the raw magnetic field;
- In the second step, we proceeded to the data processing by applying operations such as regional-residual separation, vertical and horizontal derivatives, tilt derivative, analytical signal as well as Peters half-slope and Euler deconvolution following an automatic transformation program;

- The third step was to interpret the results. At this stage, it was a question of giving a geological answer to the magnetic signatures identified on the maps produced.

III. GENERAL OVERVIEW OF THE STUDY AREA

3.1 LOCATION

The territory of Kipushi is limited to the north by the territory of Kasenga, to the south by the territory of Sakania and the Republic of Zambia and to the west by the territory of Kambove. Geographically, it is located between 27 ° and 28 ° east longitude and between 10 ° 45 "and 12 ° 30" south latitude (fig. 1).

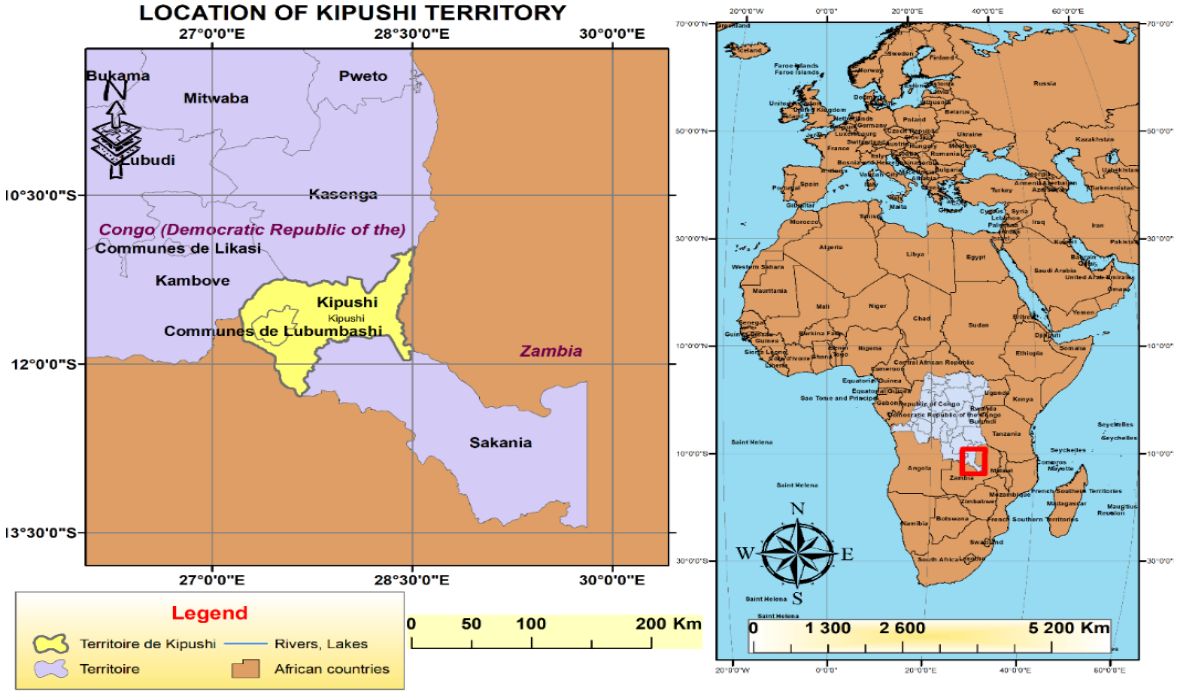

Figure 1: Location of kipushi territory.

Note that the map below shows us the part of the territory of kipushi on which we based our geophysical study (fig. 2).

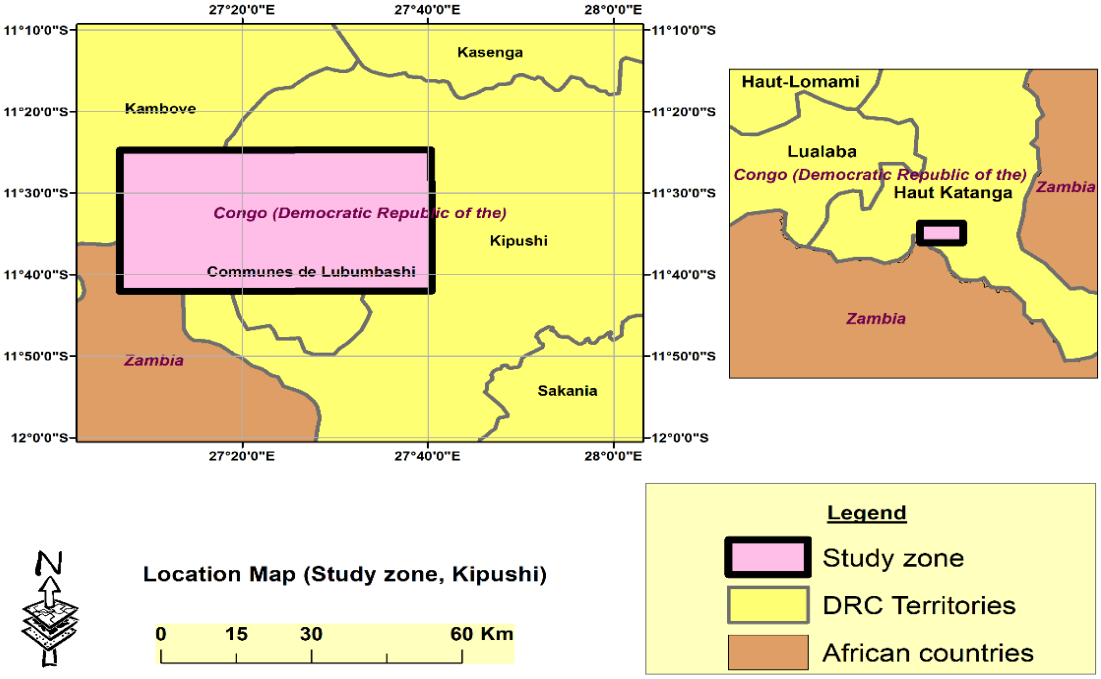

Figure 2: Location of the study area.

3.2 CLIMATE AND HYDROGRAPHY

Classified as Cw type (based on the Koppen-Geiger climate map), Kipushi enjoys a tropical climate. The average annual rainfall over the last 15 years is 1,260 mm. The annual average temperature is around 19.8 ° C. The territory is watered by several rivers and streams including the Kafubu river with a length of about 135 km which originates in the Shimpauka village of the Inakiluba group (Kaponda chiefdom) running through the territory from East to West, and flowing into the Luapula river at Kanga village of the Kinama chiefdom (one of the tourist sites in the territory). The main rivers are: Bwishibila, Munama, Musoshi, Kafubu, Kifumanshi, Kiswishi and Luapula.

3.3VEGETATION AND SOIL

The vegetation found in the territory of Kipushi is generally an open forest; the vegetation cover is mostly populated by species of the grass and legume families. The territory generally has a sandy clay soil.

3.4MAIN MINING RESOURCES IN THE REGION

3.4.1 COPPER GROUP

The copper zone contains all the stratiform cupro-cobalt and uranium deposits. The copper paragenesis covers cobalt, zinc, cadmium, lead, uranium as well as a wide range of precious and rare metals including gold, silver, germanium, barium, platinoids, etc. The Roan (R) and Kundelungu (K) sediments of this zone have undergone folding during tectonic episodes, including the Lufilian and Kundelungian phases, in a large arc (50 km wide and several hundred km long) with a concavity facing north-east. These deposits are mainly located in the R2 beam (subgroup / series of mines), in the R4 beam (Mwashya) and in the Kakontwe dolomite (Nguba).

3.4.2 TIN GROUP (TIN, WOLFRAMITE, NIOBIUM-TANTALITE, BERYL, MONAZITE)

North of Haut-Katanga, the tin belts reach a maximum width. In this favored region, the exploitation of the detrital deposits was pushed to reach the deposits in place, and it appeared rather quickly (Varlamoff, 1951 [4]) that the vein fields in pegmatitic and pneumatolytic, linked to the post-tectonic granite massifs, were distributed according to a zoogeography conforming to that indicated by Fersman in his general diagram.

3.4.3 IRON GROUP

South of the copper arc, deposits of the "iron zone" are referred to stratiform and metasomatic types. The stratiform deposits, formerly mined, consist of weakly siliceous hematite-magnetite layers (60 to 66% Fe) included in the lower Roan base quartzites (Kasumbalesa deposit) and the upper Roan Mwashya oolith upper Roan (Kanunka deposit). Metasomatic deposits have not been exploited; they form irregular clusters in the limestone levels of the Nguba near small intrusive gabbroic massifs. Mineral associations include magnetite, oligist, and pot accompanied by silica, colorless tourmaline, scapolite, corundum, and traces of copper, chromium, and nickel. The host rocks are also scapolized. Apart from Haut-Katanga, other signs were reported in the north of ex-Katanga, in Maniema and in Bas-Congo.

3.4.4 PRECIOUS METALS (GOLD, SILVER, PLATINUM)

a) Gold

In the former province of Katanga, north and south of Kalemie, we know of a series of quartz veins with pyrite, chalcopyrite, rutile and subconcordant gold in the Ruzizian schists, and gold-bearing quartz veins and veins in the chain of Kibara, northwest of Mandwe. The gold is associated in small quantities with the cupro-cobalt mineralization of the stratiform deposits of the copper arc; in Haut-Katanga, it has been observed in particular in the Kambove hill K, Kambove West, Shinkolobwe and Swambo deposits (François A., 1974 [5]). It is recovered during the refining of raw copper; some deposits are the object of artisanal mining.

b) Silver

The main silver production, 69 t in 1972, comes from the processing of silver-bearing copper and lead ores at Kipushi, with residual reserves estimated to be as high as 2,808 t. Recently, Mawson West (MW) reported the presence of silver in the Dikulushi and Kapulo deposits (Pweto territory), which may contain 513 t and 77 t respectively.

c) Platinum

In the ex-Katanga region, the association of platinum, silver, palladium and vanadium is known in the Musonoie, Ruwe and Shinkolobwe deposits. In 1953 and 1954, small amounts of platinum (875 g and 831 g) and palladium (7464 g and 4656 g) were recovered during the processing of the ore of Shinkolobwe.

IV. AEROMAGNETIC DATA

The magnetic data used in this study were collected around 1970 during the project of a high precision aeromagnetic survey carried out by the English company HUNTING on behalf of the mining company GECOMIN, currently GECAMIN Sarl for the exploration and characterization of deposits. This survey was initiated as part of the national research program, aimed at producing a three-dimensional cartography of the Katangese subsoil rich in cobalt and copper. Table 1 below shows the structure of the magnetic database obtained from the process for digitizing the magnetic map in Fig. 3. Note however that it is not easy to represent all of these data in this work following their multitude, which justifies the choice of the first 10 stations, by way of illustration.

ISSN No:-2456-2165

Table 1: Representation and structure of the aeromagnetic data used.

N° Station	Longitude (°)	Latitude (°)	Total Magnetic Intensity (nT)
01	27,1477863798	-11,4204273402	1930
02	27,1559955202	-11,4177861385	1930
03	27,1566141801	-11,4229257742	1940
04	27,1621345296	-11,4200537648	1940
05	27,1608591385	-11,4260262119	1950
06	27,1718165565	-11,4214576468	1950
07	27,157170974	-11,4298809388	1960
08	27,1639762324	-11,4295954034	1960
09	27,1706387233	-11,4292146897	1960
10	27,1615491822	-11,4319034806	1970

Note that the data shown in the table above come from the magnetic map carried out during the aeromagnetic survey of 1970 by the English company HUNTING on behalf of GECOMIN. This aeromagnetic map has been cut into 15 sheets. Figure 3 below shows us the map from sheet 2 used as a base map for this work.

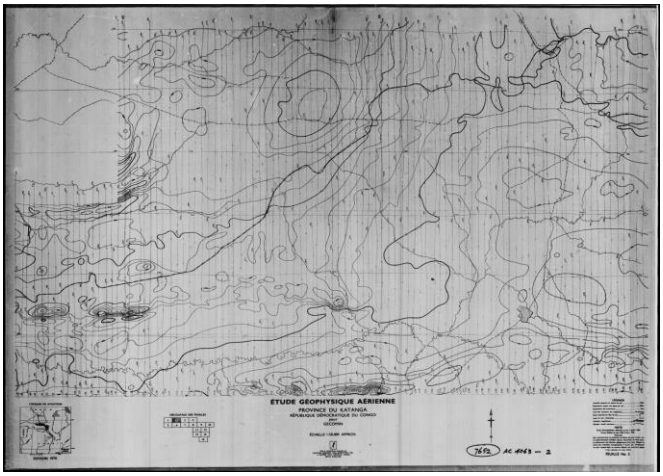

Figure 3: Magnetic contour map of the study area (carried out by HUNTING in 1970).

V. DATA PROCESSING

The geological interpretation of magnetic data is facilitated by filtering the data through various mathematical filters. The various operations that we used to carry out this study are:

- **Digitization** of the entire 1/50000 magnetic contour map automatically using the Surfer software. Either in total plus or minus 2500 points have been stored as raw magnetic field data;
- **The Reduction To Pole (RTP)** taking into account the local parameters of the terrestrial magnetic field obtained thanks to the geomagnetic model IGRF (International Geomagnetic Reference Field) of 1970 in the Haut-Katanga. This operation eliminates the distortions of the anomalies in order to obtain those whose maximum is centered on the magnetic sources;
- **Regional-residual separation** in order to attenuate the regional field from deep structures in order to enhance residual anomalies for the identification of structures generally located in the sediment cover;
- **The vertical and horizontal derivatives** which respectively allow us to identify lineaments and better understand the position of the bodies that create the anomalies located near the surface;
- **The tilt angle** which puts in relation the relation between the first vertical derivative (z) and the total of the horizontal derivatives (x and y). This value therefore represents the angle between the total horizontal derivative (x, y) and the first vertical derivative (z). This transformation makes it possible to highlight relatively shallow bedrock structures and also certain targets of interest for mineral exploration while eliminating the regional gradient (Lafleche, 2010 [6]);
- **The analytical signal** which is the sum of the vertical and horizontal gradients of the residual magnetic field. It is useful in locating the boundaries of source magnetic bodies, in particular where remanence or low magnetic latitude complicates the interpretation (Abdennacer CHANAOUI and al., 2016 [7]);
- **The Peters half-slope method** to have a direct estimate of the depth of the dykes identified on the residual magnetic map; and
- **Euler's deconvolution** for automatic localization of faults, contacts and dykes.

\

Figure 4 below shows us the workflow for data processing.

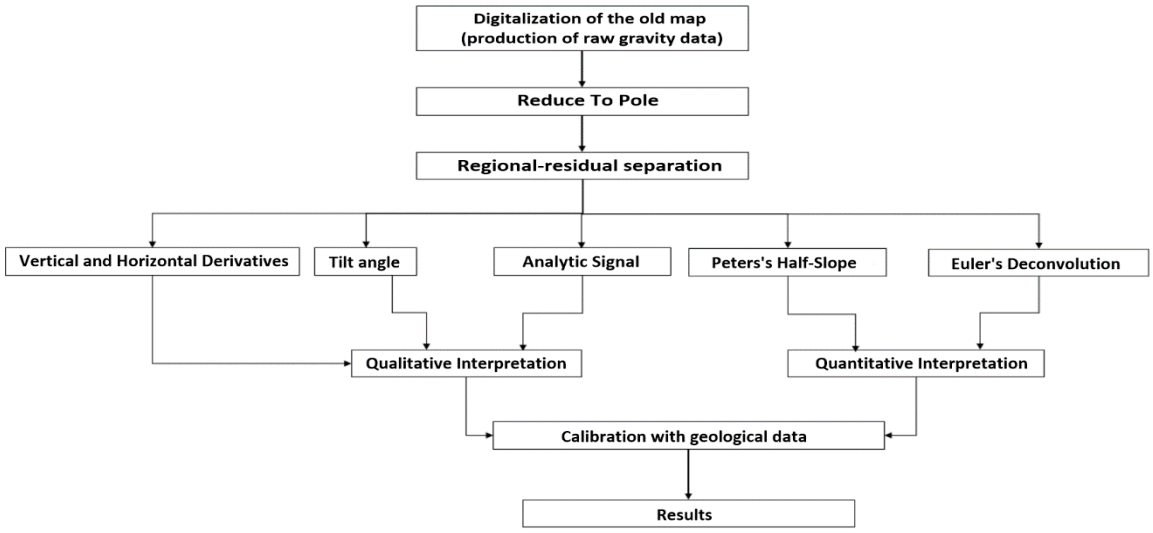

Figure 4: Workflow for data processing.

VI. INTERPRETATION OF THE RESULTS

6.1.1 TP MAP

Total Magnetic Intensity (TMI) values were reduced to the pole (RTP) using the 1970 International Geomagnetic Reference Field (IGRF) geomagnetic model in an attempt to bring them back in line with their sources. The following figure shows us the difference between the TMI map and the RTP map (fig. 5 a and b).

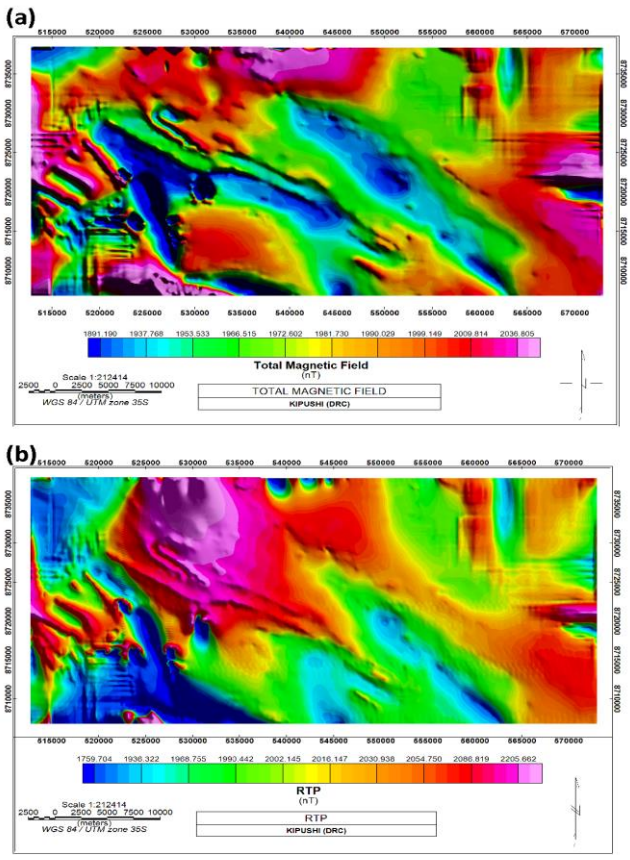

Figure 5: (a) TMI map; (b) RTP map.

The RTP map is dominated by the presence of positive anomalies, the most important of which is a dome-shaped anomaly located in the north of the study area. This anomaly indicates the presence of a body of high magnetic susceptibility at this location. In the southwest, a low intensity anomaly indicating the presence of diamagnetic bodies.

6.1.2 MAGNETIC RESIDUAL MAP

The magnetic residual map shows us small local disturbances of the magnetic field which are secondary in size but essential in the study of geological structures. The sources that generate this type of anomalies are generally shallow geological structures (mineral deposits, near-surface faults, folds, salt domes, cavities, magmatic intrusions, etc.). The magnetic residual map has anomaly values ranging from -62 and 41 nT, it also reveals significant anomalies that we can characterize based on their shape, orientation and intensity (Fig. 6).

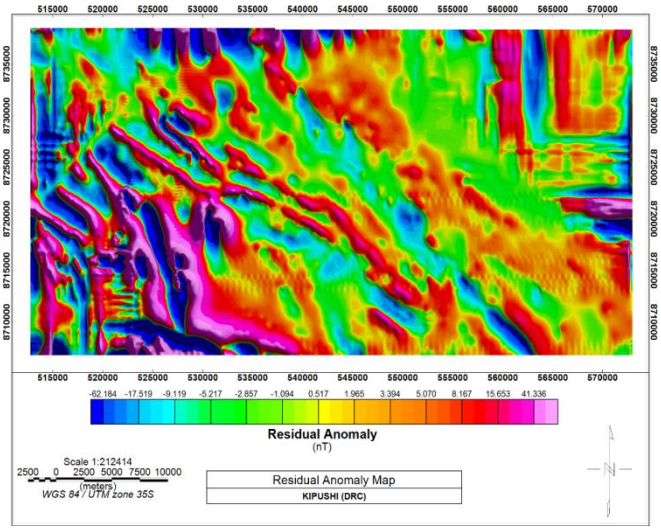

Figure 6: Magnetic residual map.

ISSN No:-2456-2165

On this map we notice the presence of high intensity magnetic lineaments covering the western and central parts. In the western part, in particular, abrupt variations in anomalies are observed, a phenomenon which testifies to an intense shear zone caused by the various tectonic episodes that this zone has undergone. Note also the attenuation of the dome-shaped anomaly north of the study area. This type of anomaly indicates the presence of geological structures containing mineral substances of high magnetic susceptibility, such as most of the metal ore deposits found in this area. The preferred structural direction of these anomalies is NW-SE. These magnetic lineaments are therefore important targets in mining exploration. Note also that a magmatic intrusion into the sedimentary column could generate similar positive anomalies.

As for the anomalies of medium and / or low magnetic intensity, they spread to the East creating significant contrasts of anomalies in this area. These negative anomalies reveal the presence of synform structures, mineral substances of low magnetic susceptibility such as salt domes. Geophysically speaking, a mass of salt is generally diamagnetic and produces low negative magnetic anomalies which are most often masked by a more intense phenomenon (para or ferromagnetic rock cap). The anomalies related to salt domes appear positive if they have a cap of mafic volcanic rocks and negative or zero if they do not (Géophysique Camille St-hilaire, 2015 [8]). In addition, the salt is generally lighter than the surrounding rocks. As a result, there will be a negative density contrast which will have the effect of locally reducing the intensity of gravity anomalies. Thus, negative circular gravity anomalies are generally observed above salt domes. Some examples such as the "Way dome" in the Gulf of Mexico and the "Grand Saline dome" in Texas should be noted (G. R. Foulger et al., 2002 [9]).

6.1.3 VERTICAL AND HORIZONTAL DERIVATIVE MAPS

Calculating vertical derivatives can attenuate long wavelengths and significantly improve the resolution of smaller anomalies near the surface. Applying this filter to the magnetic data amplified the effect of shallow sources by attenuating the effect of deep sources, and further delineated the geometric boundaries of bodies. Figure 7 below shows the map of the first vertical derivative of the magnetic anomaly.

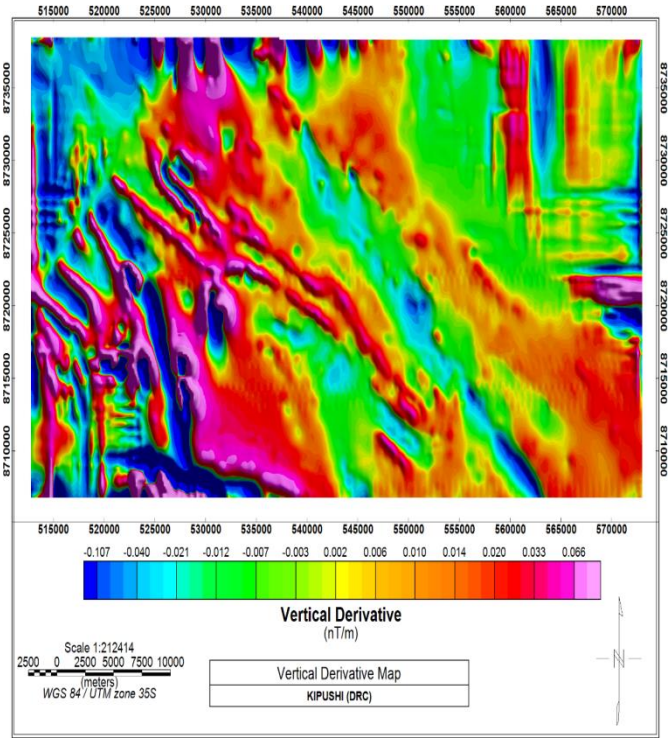

Figure 7: Map of the first vertical derivative.

We find that like residual anomalies, the first vertical derivative map shows several positive and negative linear anomalies. The magnetic dome of the northern part as well as the magnetic depression of the southwest clearly visible on the RTP map disappear to give way to anomalies of small extension whose sources are certainly shallow.

Horizontal gradient maps identify all areas of anomaly contrast and present them as maxima. It should be noted that the calculation of a horizontal gradient in a given direction makes it possible to bring out all the lineaments of said zone in a direction almost perpendicular to that of the applied filter. Thus, in order to highlight a maximum number of lineaments in our study area, horizontal derivative filters of RTP magnetic anomalies along the X and Y directions were applied (fig. 8 a and b).

ISSN No:-2456-2165

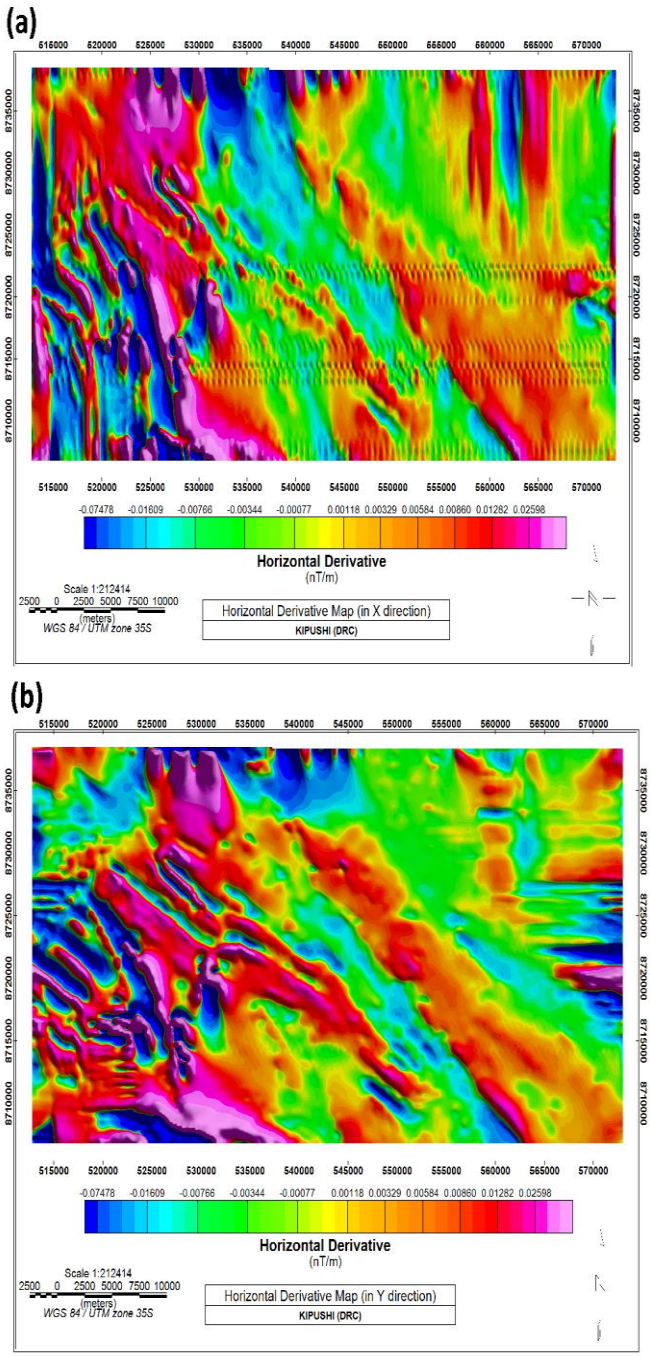

Figure 8: (a) Horizontal Derivative in X direction; (b) Horizontal Derivative in Y direction.

The visual analysis of the above maps allows us to vectorize the magnetic lineaments revealing the presence of several major tectonic accidents such as faults or lateral lithological contacts.

6.1.4 TILT DERIVATIVE MAP

This operator is defined as the tangent arc of the ratio of the vertical derivative of the total field to the modulus of its horizontal gradient (Brahimi Sonia et al., 2008 [10]). Figure 9 below shows the Tilt Derivative map.

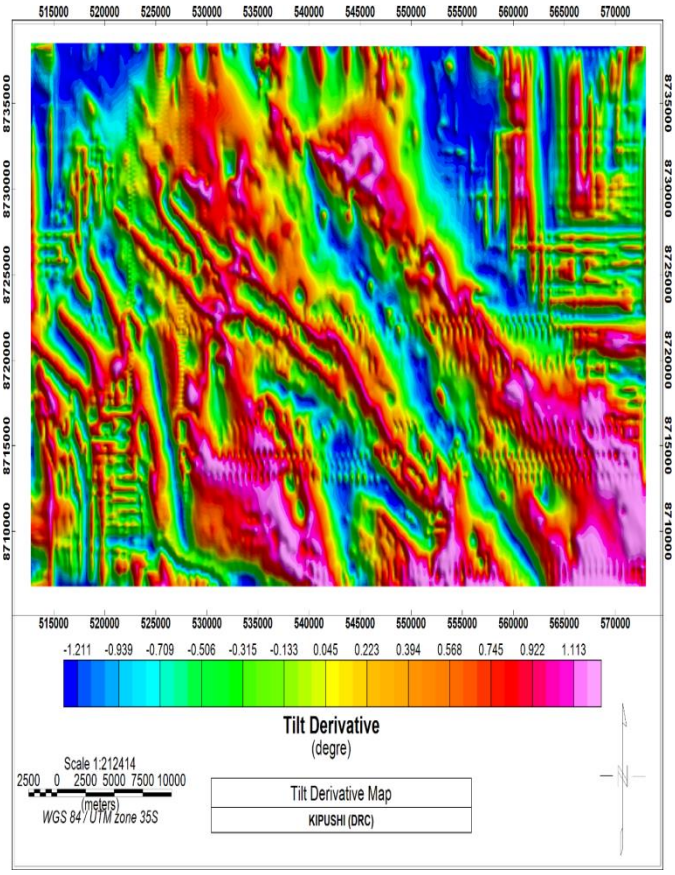

Figure 9: Tilt Derivative map.

On this map, the linear positive anomalies are well individualized, especially in the central part of our study area. These give us important information on the NW-SE direction of the shallow lineaments which can be considered as faults, dykes or veins which are interesting targets in mineral exploration.

6.1.5 ANALYTICAL SIGNAL MAP

Using another digital filter, it is also possible to calculate what is referred to as the Analytical Signal. It is therefore the sum of the vertical and horizontal gradients of the residual magnetic field. Its properties are quite exceptional. It therefore combines the horizontal and vertical derivatives and creates peaks above the borders of large anomalies or in the center of small ones. This type of filter facilitates the identification of lineaments and bodies of quasi-circular geometry that are difficult to identify by other digital filters (fig. 10).

ISSN No:-2456-2165

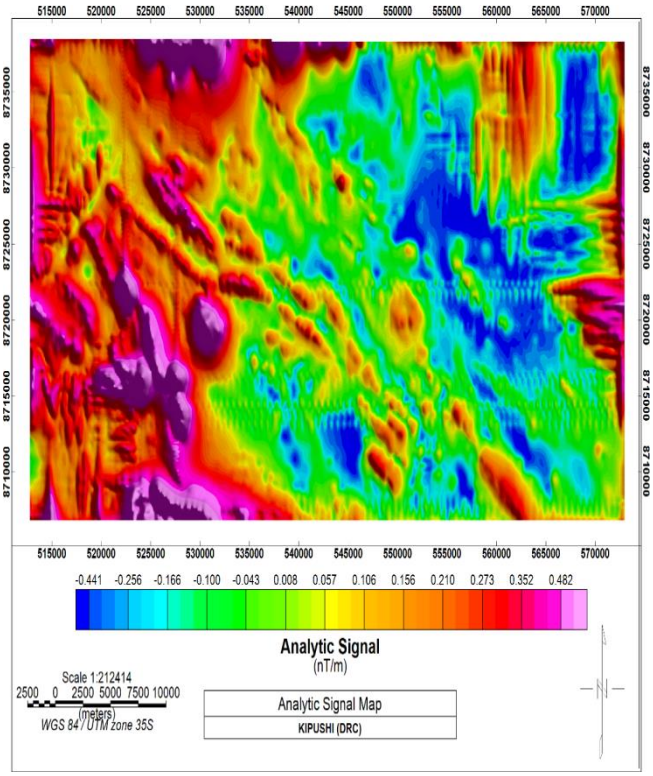

Figure 10: Analytical Signal map.

This map shows a large contrast of anomaly dividing the area into two areas:

- The West domain characterized by a positive analytical signal. In this area, we find quasi-circular positive anomalies which indicate the presence of folding zones formed by compressive movements or concentrations of mineral substances of high magnetic susceptibility such as most of the metal ore deposits present in this area. Note also that a magmatic intrusion in the sedimentary column could generate a similar analytical signal;
- The East domain characterized by a negative analytical signal with very slow spatial variation of the anomalies. This may be due to a subsidence of the magmatic or metamorphic basement.

6.2 QUANTITATIVE INTERPRETATION

6.2.1 ESTIMATE OF THE DEPTH OF SOURCES BY THE PETERS HALF-SLOPE METHOD

We used the Peters half-slope method to have a direct estimate of the depth of the dykes identified on the residual magnetic map. This method consists in drawing a certain number of segments tangent to the profile. The desired quantity is the horizontal distance also called the Peters distance h between the two points tangents to the magnetic profile as shown in the diagram below (fig. 11).

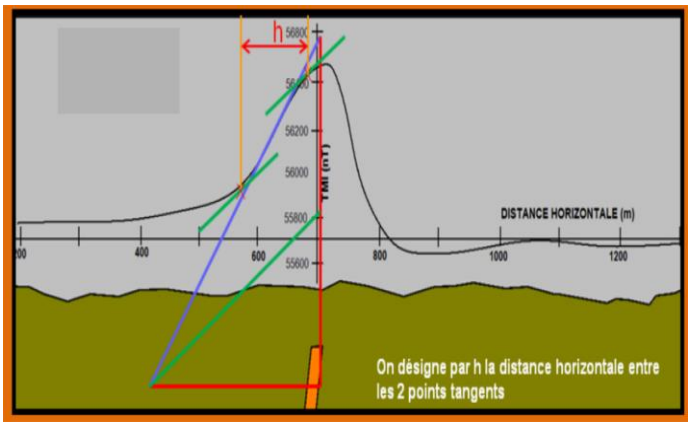

Figure 11: Diagram of the direct calculation of the depth of a dyke using the Peters half-slope method (Géophysique Camille St-hilaire, 2015 [8]).

After calculating h, the depth H of the dyke is then obtained by the following equation:

$$H = \frac{h}{n} \qquad (1)$$

To evaluate n, we use the shape of the curve:

- For an acute curve, we choose n = 1.2;
- For a moderately sharp curve, we choose n = 1.6;
- For a curve clearly showing a plateau, we choose n = 2.

This method requires the tracing of profiles. Thus, during the interpretation, the residual magnetic profiles A and B were made to obtain either depths or other useful data. The objective here is to collect as much information as possible on the depth of the geological structures of interest. The location of these profiles is presented as a whole in Figure 12.

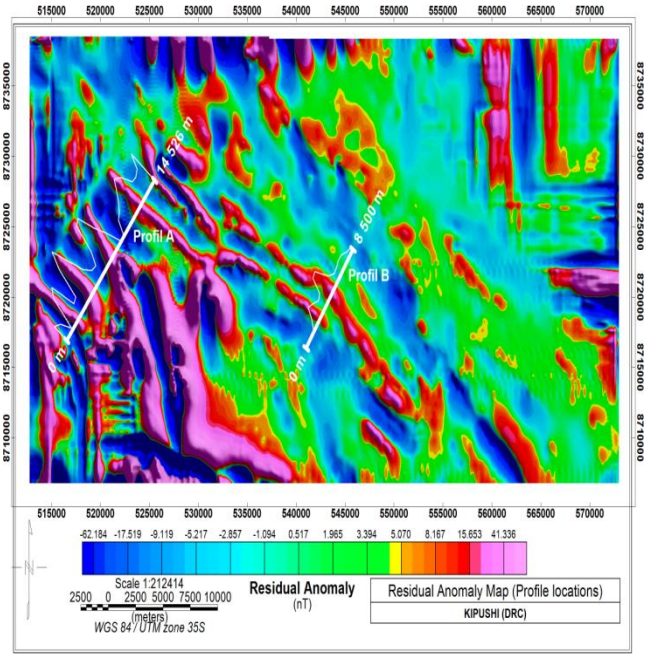

Figure 12: Map of the location of the different profiles (in white).

ISSN No:-2456-2165

Profile A has a length of 14,526 m and is oriented in the NE-SW direction (fig. 13 a). It intersects perpendicularly a series of abrupt variations of anomalies clearly reflecting an intense deformation to the west of the study area. On this profile, four positive anomalies were identified and interpreted as being dykes. Profile B has a length of 8,500 m and is also oriented in the NE-SW direction, thus intersecting the long dykes located in the central part of this zone (fig. 13 b).

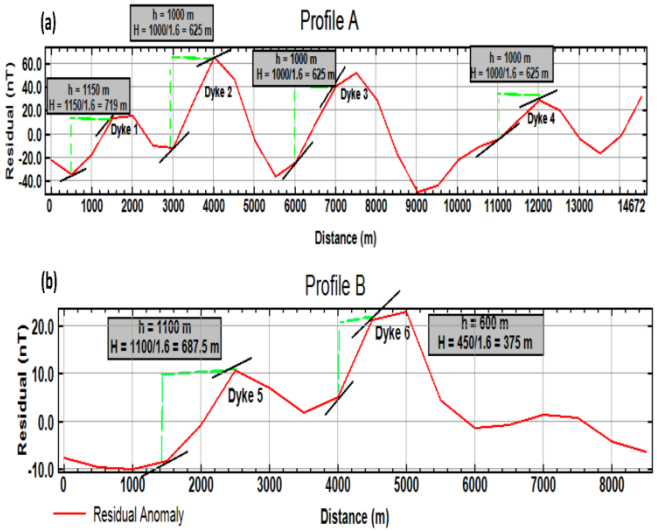

Figure 13: Estimation of the depth of the sources by the Peters half-slope method. (a) Profile A; (b) Profile B.

Apart from dyke 1 which has an estimated depth of 719 m, we found a depth of 625 m for dykes 2, 3 and 4 intersected by profile A. As for dyke 5 and 6 crossed by profile B, they respectively a depth of 687.5 and 375 m. Table 2 below summarizes all the depth values obtained for the dykes.

Table 2: Depth of the identified dykes.

	Profile A				Profile B	
Features	**Dyke 1**	**Dyke 2**	**Dyke 3**	**Dyke 4**	**Dyke 5**	**Dyke 6**
Peters distance h (m)	1 150	1 000	1 000	1 000	1 100	600
Depth H (m)	719	625	625	625	687,5	375

6.2.2 ESTIMATE OF THE DEPTH OF SOURCES BY THE EULER DECONVOLUTION METHOD

The automatic localization of sources by Euler's deconvolution, for structural indices of N = 0 for the identification of faults or contacts and N = 1 for the identification of dykes, allowed to have a better insight on the depth of sources. Figures 14 and 15 below show us respectively the maps of Euler's solutions for structural indices of N = 0 and N = 1 on an analytical signal background. These maps are provided with their histograms representing the statistical distribution of the depths of the sources of Euler's solution.

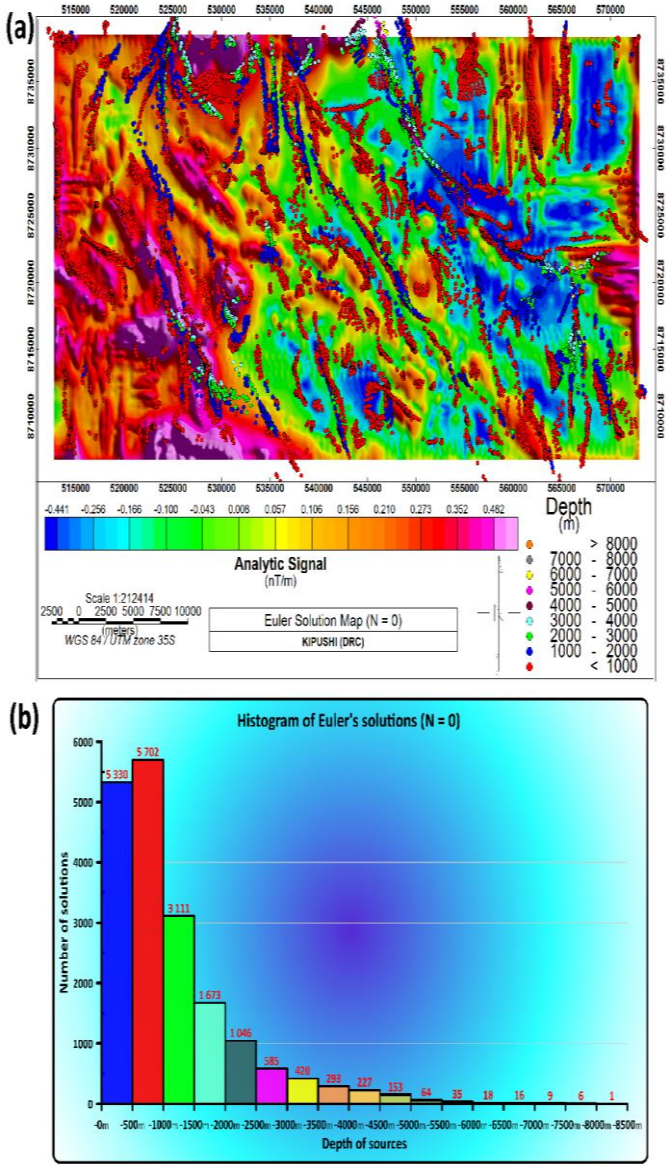

Figure 14: (a) Euler solutions obtained with a structural index N = 0; (b) Histogram of Euler's solutions obtained with a structural index N = 0.

On the map above, the solutions found are also oriented for the most part in the NW-SE direction. Most of these structures are located at depths ranging from 0 to 1500 m, while few solutions have been found beyond this depth. Note however that the histogram above shows us that a solution was found at depth greater than 8000 m. Geologically speaking, these solutions represent either faults caused by tectonic events or lateral contacts between geological formations.

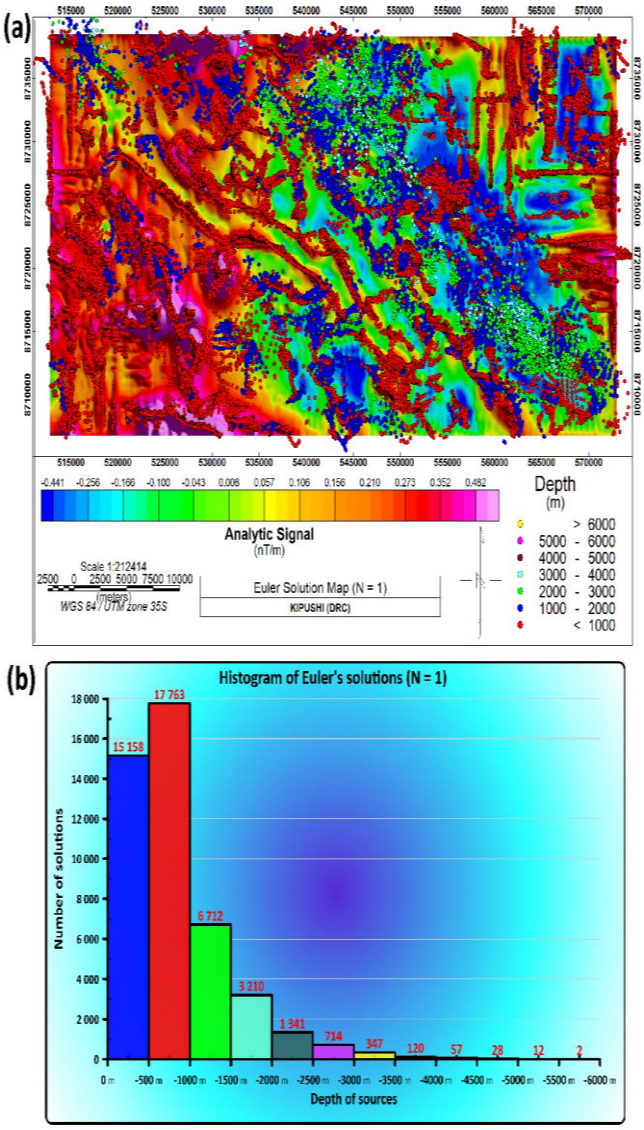

Figure 15: (a) Euler solutions obtained with a structural index N = 1; (b) Histogram of Euler's solutions obtained with a structural index N = 1.

The processing of Euler's deconvolution with a structural index of 1 for the localization of dyke-shaped structures gives us more solutions than that of the structural index of 0. On the map above, we see an alignment of the solutions on large positive and negative linear anomalies. The map and the histogram also show us a predominance of solutions located at shallow depth (<1000 m), especially for linear and quasi-circular anomalies in this area. Bodies deeper than 1000 m are found in large proportion in the eastern part of the zone but also in the western part in low proportion. Like the map of N = 0 solutions, we find that the localized structures also have a preferential direction of NW-SE.

The 3D models of Euler's solutions for N = 0 and N = 1 only improve the visual analysis of all the structures described on the previous maps (fig. 16).

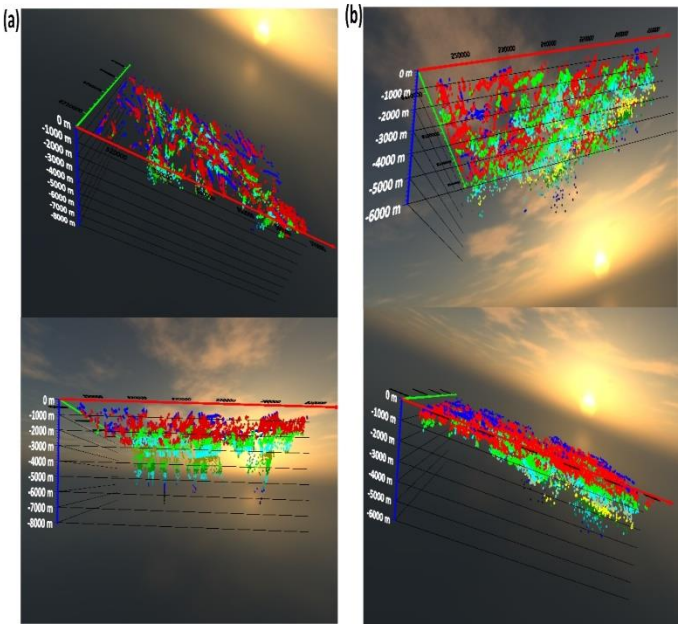

Figure 16: 3D visualization of the position of the sources of Euler's solution. (a) N = 0; (b) N = 1.

6.3 CALIBRATION OF MAGNETIC DATA WITH THE GEOLOGICAL DATA AND DISCUSSION

Our study area is located in the Katanga supergroup, more precisely in the Katanga copper arc which is world famous for its important copper and cobalt mineralization. Recent studies on the lithostratigraphy of the DRC published by Fernandez Alonzo et al., 2015 [11] divide the sedimentary successions of the Katanga Supergroup, with a total thickness of 5 - 10 km, into 3 lithostratigraphic units; from top to bottom:

- **The Kundelungu Ku Group** (formerly the Superior Kundelungu) is made up of 3 Sub-groups: - Biano (Ku 3) formed of arkoses, conglomerates and clayey sandstones, argillaceous lithology; -Ngule (Ku 2) which is essentially dolomitic with intercalations of sandstones and clays; - Gombela (Ku 2) formed by a small conglomerate at the base (Kyandamu formation) and Oolithic limestone at the top (Lubudi formation);
- **The Nguba Ng Group** (formerly the Lower Kundelungu + Grand Conglomerat) is divided into two Sub-groups: the Muombe Sub-group (Ng 1), a carbonato-siliciclastic mixture and the Bunkeya Sub-group (Ng 2), predominantly siliciclastic. The base of the Muombe is formed by the glaciogenic conglomerates of the Mwale formation, better known as the 'Grand Conglomerat'. The "carbonate capes" capping the Mwale formation (Kaponda, Kakontwe and Kipushi formations) contain Zinc – Lead– (Copper) deposits in the Congo;
- **The Roan R Group** begins with a basal siliciclastic unit (Mindola / RAT subgroup of argilo-talcous rocks R1), followed by a carbonate and siliciclastic unit (Subgroup Kitwe / Mines R2) and a carbonate unit (Kirilabombwe / Dipeta R3 sub-group). Lepersonne's (1974) [12] Mwashya, redefined as a Subgroup of Mwashya R4, is considered by most geologists to be the top of the Roan Group. Others however consider it either as a Group

ISSN No:-2456-2165

distinct from the 3 others above the Roan, or as a Sub-group of the Nguba Group. The Roan Group is present in Zambia and DRC, the 2 higher units only in DRC. Note that Groups R2 and R3 contain significant copper and cobalt mineralization in the DRC. The cupro-cobalt deposits of the R2 Mining Subgroup are the most important in terms of both tonnage and grade. These are stratiform copper mineralizations included mainly in carbonate series.

From the regional geological map of the DRC, we digitized the main lithostratigraphic units of the Katanga Supergroup to produce a simplified geological map of our study area (fig. 17).

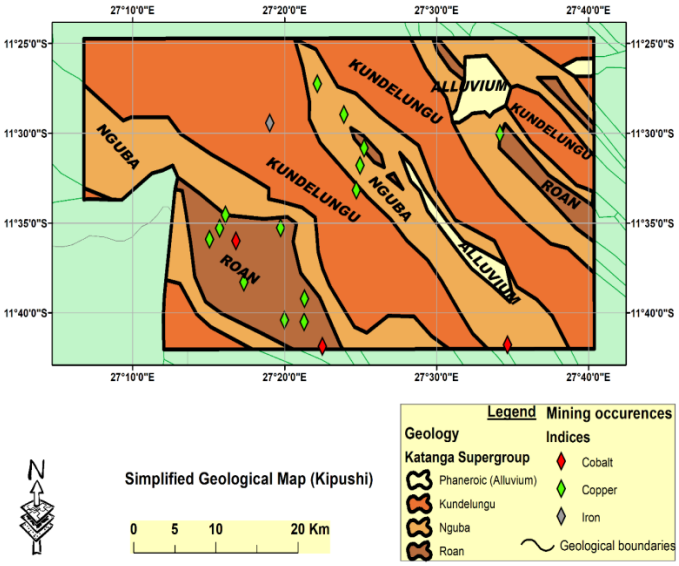

Figure 17: Simplified geological map of the study area (digitized from the geological map of the DRC published by Fernandez Alonzo and al., 2015 [11]).

Superimposing geological data on the magnetic residual map reveals important information about the structural and stratigraphic geology of this region (Fig. 18).

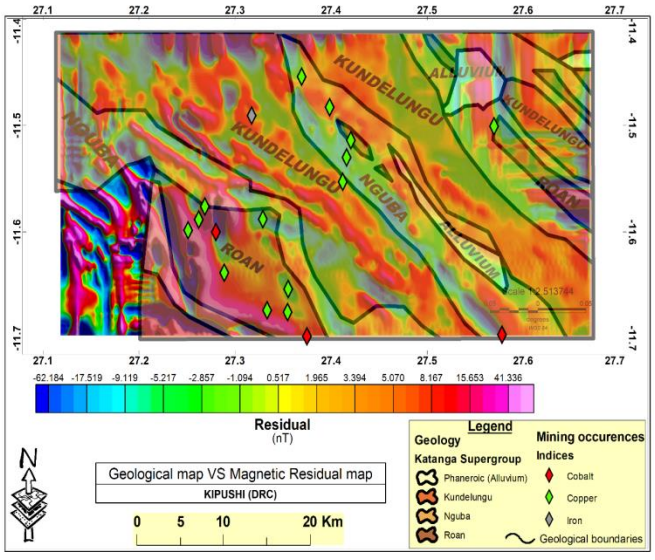

Figure 18: Geological map superimposed on the magnetic residual map of the study area.

The analysis of the map of the superposition of geological data to the residual magnetic anomalies above, allows us to highlight several observations that improve our knowledge of the geology of this area. The preferential orientation of the NW-SE magnetic anomalies correlates perfectly with that of the geological formations present in this area.

The Roan group, the largest portion of which is located in the South-West, is characterized by a higher magnetic intensity than that of the other Groups. This is explained by the fact that being at the base of the Katanga Supergroup, the Roan Group rests directly in discordance above crystalline basement that have undergone the Kibarian orogeny (J. Cailteux, 1974 [13]). The latter are magmatic and metamorphic rocks which generally have a much higher susceptibility than that of sedimentary rocks. This strong magnetic intensity could therefore come from the rise of the dome-shaped crystalline basement near the surface at this location. Magmatic intrusions would also cause similar positive anomalies. In this area, the dyke depth estimated by the Peters half-slope and Euler deconvolution methods is less than 1000 m.

It should be noted that the importance of the uplifts of the dome-shaped crystalline basement in the genesis of copper mineralization in the Roan Group was the subject of a study carried out in the Kinsenda copper deposit which rests in discordance on the granite dome of Luina (near Kasumbalesa) (Kyalwe NGOYI and al., 1997 [14]). According to this study, the mineralization of the Subgroup of the R2 Mines could come in particular from the leaching of the basement which consisted of igneous and metamorphic rocks and probably also of copper porphyries. This therefore explains the presence of several mining occurrences in this Group in our study area.

Magnetic intensity is medium in the rocks of the Nguba Group while it is medium and / or high in the Kundelungu group located in the center of this area. This group is characterized by a long dyke (dyke 6) of about 24 km, the depth of which has been estimated on profile B at 375 m by the Peters half-slope method and at 452 m by the deconvolution method of Euler (fig. 19).

ISSN No:-2456-2165

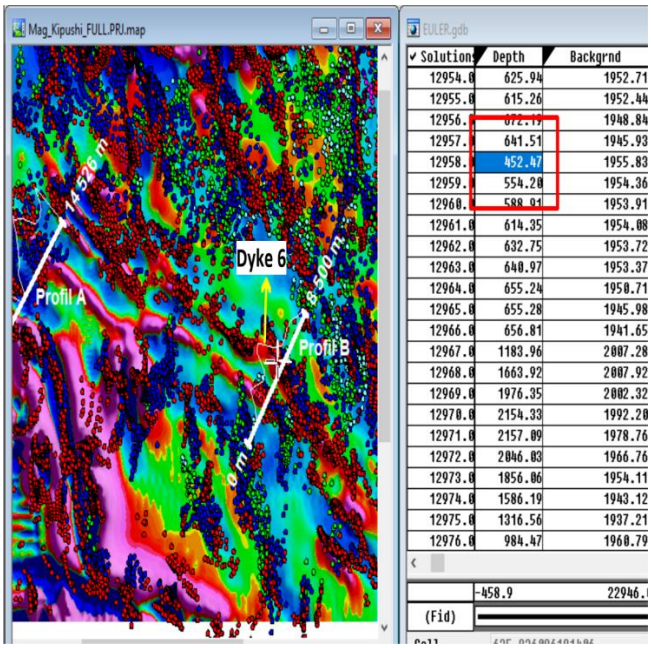

Figure 19: Location of dyke 6 on the map of Euler's solutions N = 1.

The qualitative and quantitative interpretation of the magnetic data by integrating geological data has enabled us to establish a structural map on which all the lineaments highlighted by the different processing methods have been represented (fig. 20).

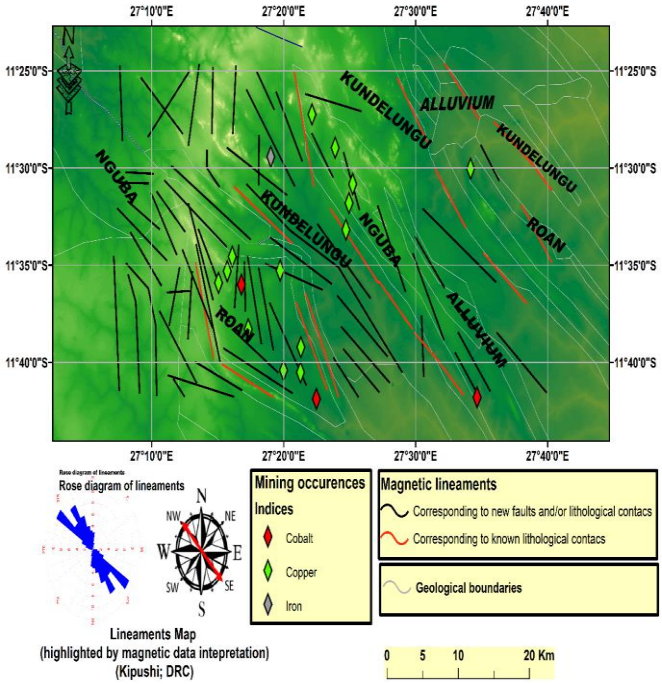

Figure 20: Structural map of the study area.

On this map, the black lineaments correspond to new faults and / or lithological contacts enhanced by magnetic interpretation and the red lineaments correspond to known lithological contacts. The rose diagram shows us that the preferential direction of the lineaments is NW-SE. The Katanga Supergroup was subjected to the Lufilian tectonics which folded the sediments in an east-west arc 500 km long (Lufilien arc). This tectonic event in addition to the Kibarian orogeny which affects the basement of sedimentary rocks therefore have the basis of these multiple lineaments highlighted by the magnetic data. It should also be noted that the western part, in particular the Roan Supergroup in the South-West, seems strongly sheared because there are a large number of lineaments there, while the eastern part is covered by very few lineaments. These new lineaments which bring lithological units into contact in this region open the way to new prospects for the discovery of new mineral deposits in this zone, whose copper, cobalt and zinc reserves are immense.

VII. CONCLUSION

This study focuses on the Kipushi region in the Haut Katanga Province in the Democratic Republic of Congo where mining activity is highly developed in the exploitation of deposits of Zinc, Lead, Copper, Cobalt, Iron, etc. The reinterpretation of the aeromagnetic data obtained by Hunting in 1970, brings in the sector which concerns us some interesting complements to the geological cartography. As a result, we noticed that the NW-SE orientation of the lithostratigraphic units was confirmed thanks to the calibration of the magnetic data with the regional geology and the establishment of the rose diagram of the highlighted structures. Analysis of residual anomalies and vertical and horizontal gradients shows us that the Roan Group, which is also the most mineralized in the Katanga Supergroup, appears to be more sheared than the Nguba and Kundelungu Groups because there are a large number of lineaments. Note also that strong contrasts of anomalies have been identified along known lithological contacts in the region. These sudden variations in magnetic susceptibility, which are clearly visible as positive gradients on the vertical and horizontal derivative maps and on the tilt angle map, could be closely related to the mineralization observed in this region. The methods of quantitative interpretations such as the Peters half-slope performed along profiles A and B as well as the Euler deconvolution performed with histograms allowed us to estimate the depth of the majority of dykes, faults and contacts. less than 1000 m. The new structural map produced enriches the regional geological map with new structures which must be the subject of field studies.

REFERENCES

[1]. François, A. (2006), La Partie centrale de l'arc cuprifère du Katanga : étude géologique. MRAC, Tervuren African Geoscience Collection, n° 109.

[2]. Cellule Technique de Coordination et de Planification Minière (CTCPM) (2003), Guide de l'investisseur du secteur des mines et hydrocarbures de la R.D. Congo.

[3]. Jean Omasombo Tshonda, (2018), Haut-Katanga : Lorsque richesses économiques et pouvoirs politiques forcent une identité régionale, Tome 2 : bassin du cuivre : matrice et horizon, MRAC, Tervuren.

[4]. Varlamoff N. (1951), Types de gisements de cassitérite du Maniema et du Ruanda. In Congrès scientifique d'Elisabethville, Comptes rendus, vol. 2, t. 2, pp. 409-431.

[5]. François, A. (1974), Stratigraphie, tectonique et minéralisations dans l'arc cuprifère du Shaba (République du Zaïre), Annales de la Société géologique de Belgique, publications spéciales), pp. 79-101.
[6]. Marc Richer-LaFlèche (2010), Levés gravimétrique et de résistivité électrique sur la propriété Témiscouata.
[7]. Abdennacer CHANAOUI and Messaouda BAKHALED (2015), Interprétation des données aéromagnétiques de
[8]. Khemis Miliana, Université de KHEMIS MILIANA, Faculté des Sciences et de la Technologie, Département des Sciences de la Matière, République Algérienne Démocratique et Populaire.
[9]. Géophysique Camille St-hilaire (2015), Interprétation des données : Rapport Final, Ministère de l'Energie et des Ressources Naturelles, Quebec.
[10]. G. R. Foulger and C. Peirce (2002), Geophysical methods in geology, p. 27.
[11]. Brahimi Sonia, Munschy Marc, Bourmatte Amar (2008), Apport de la gravimétrie et du magnétisme à l'étude de la structure du bassin d'Illizi (Algérie).
[12]. Fernandez Alonzo and al., (2015), Carte Géologique de la République Démocratique du Congo au 1/2.500.000: Notice explicative, Ministère des Mines, République Démocratique du Congo.
[13]. Lepersonne, J (1974), Carte géologique du Zaïre au 1/2.000.000: Notice explicative, Département des mines, Direction de la Géologie, Kinshasa, République du Zaïre.
[14]. J. CAILTEUX (1974), Minerais cuprifères et roches encaissantes a Musoshi, province du shaba, République du Zaïre. Annales de la Société Géologique de Belgique, T. 96, 1973, pp. 495-521.
[15]. Kyalwe NGOYI and Léon DEJONGHE (1997), Géologie et genèse du gisement stratoïde cuprifère de Kinsenda (SE du Shaba, Zaïre) Bulletin de la Société belge de Géologie, T. 104 (3-4), 1995, pp : 245-281